(Preprint) AAS 13-XXX

TRAJECTORY ERROR AND COVARIANCE REALISM FOR LAUNCH COLA OPERATIONS

M.D. Hejduk,[*] D. Plakalovic,[†] L.K. Newman,[‡] J.C. Ollivierre,[§] M.A. Hametz,[**] B.A. Beaver,[††] R.C. Thompson[‡‡]

Non-uniform guidance and practices for launch collision avoidance (LCOLA) among different NASA field centers (and the Air Force launch ranges) has prompted NASA Headquarters to commission a study to develop recommendations for standardizing the process and to issue suggested screening thresholds. The full study should be completed in early 2013, but the results for the initial phases are reported herein, namely an investigation of the accuracies of the pre-launch predicted trajectories and the realism of their associated covariances. The study determined that, for the Atlas V and Delta II launch vehicles, trajectory errors remain about an order of magnitude larger than General Perturbations (GP) satellite catalogue errors, confirming that it is not necessary to resort to a precision catalogue in order to perform LCOLA screenings. The associated launch covariances, which are large and had been thought to be conservatively sized, were found instead to be quite appropriately determined and fare well in covariance realism analyses. As such, the launch-related information feeding the LCOLA process will allow a durable calculation of the probability of collision and thus can serve as a reliable basis for LCOLA operations.

INTRODUCTION

While Launch Collision Avoidance (LCOLA) has been a standard launch range practice at some level for more than a decade, at present there is neither a requirement nor standardized process for LCOLA across the Agency. NASA's Launch Services Program (LSP) for Expendable Launch Vehicles (ELVs) at NASA Kennedy Space Center (KSC) provides LCOLA analysis to NASA's robotic missions if either requested or required by the spacecraft customer. LSP works with the Aerospace Corporation to perform these functions, as Aerospace also performs similar functions for Air Force missions. The NASA Human Spaceflight Mission Control Center (MCC) team has also provided limited pre-launch conjunction screening for the Shuttle. The process is indeed decentralized, with several different organizations performing calculations and providing support in different ways.

[*] a.i. solutions, Inc. 985 Space Center Dr., Suite 205 Colorado Springs, CO 80915
[†] a.i. solutions, Inc. 985 Space Center Dr., Suite 205 Colorado Springs, CO 80915
[‡] Mail Code 595, NASA Goddard Space Flight Center, 8800 Greenbelt Road Greenbelt, MD 20771
[§] NASA/KSC address
[**] NASA/KSC address
[††] NASA/KSC address
[‡‡] Aerospace address

Launch Collision Avoidance Screening Methodologies

Initially, LCOLA screenings used solely a miss distance approach; and in many cases, this technique is still used today. The miss distance method is a comparison of the nominal trajectory of the launched object(s) versus each object in the resident space object catalog. At each integration step in the trajectory, the point-to-point distance between the objects is computed; and if the minimum distance between a launched object and an on-orbit object is within the evaluation criteria volume, then the vehicle is unable to launch at that evaluated launch time. For different object types, such as manned assets, active payloads, dead payloads, rocket bodies, and debris, different miss distance criteria may be used to determine if there is a conjunction violation. The advantages of the miss distance technique are the relatively simple required data inputs and the speed of the screening runs: only the nominal launch trajectories of the vehicle and separated objects are required (*i.e.*, no covariance data are needed), and the calculation at each integration step is a simple comparison rather than a complex numerical integration. This speed and convenience, however, comes at a price. Since the nominal trajectory is all that is considered, the inherent problem is that a vehicle will never fly exactly to the nominal trajectory. To compensate for the lack of a statement of trajectory error (usually packaged as a covariance), it is necessary to set the allowable miss-distance thresholds to larger values, which often results in a proliferation of conjunction violations and the excessive closure of launch windows. This drawback is dramatically highlighted when comparing liquid-fueled to solid-fueled engines. For a launch vehicle that consists of all solid propulsion motors, all engine propellants must be consumed, necessitating the use of energy scrubbing techniques to dissipate excess energy in order to minimize injection errors. Energy scrubbing is well known to result in much higher trajectory variations in flight as compared to liquid propulsion systems, which can be shut down when the desired orbit targets have been achieved. However, this sort of system-dependent variation in capabilities is generally not captured in miss distance evaluations or thresholds.

To account for these expected variations during flight, a Probability of Collision (P_c) method has become more widely utilized, as it allows for a higher fidelity launch vehicle representation and a more accurate measure of risk. The probability of collision associated with a given on-orbit conjunction is a function of three parameters: the effective collision area (which quantifies the sizes of the objects), the nominal closest approach distance, and the uncertainties in the positions of the objects. In this computation, the P_c is determined for each conjunction using the covariances of the objects (as an expression of position uncertainty) to determine the likelihood that both objects will be at the same location at the time of closest approach. More inputs are required for this calculation than for the miss-distance method, and it is more computationally intensive; but the yield is an actual probabilistic statement of collision risk, which requires no hedging or inflation of thresholds in order to compensate for unexpressed errors.

The launch vehicle covariances have been a source of significant concern within the LCOLA community. As the relative size of the launch vehicle one-sigma position ellipsoid has been believed to dwarf the variability ellipsoid of the on-orbit objects, it is the accuracy of the launch vehicle covariance that most influences the overall accuracy of the LCOLA P_c calculations. There has been concern that the covariances for the launch vehicle are overly conservative and thus do not represent actual vehicle performance. This issue is explicitly addressed in the present investigation.

Launch Collision Avoidance Policies

Prior to February 2010, the launching Range would screen each launch attempt against only manned/mannable objects, such as the International Space Station (ISS), the Space Shuttle, and Soyuz spacecraft. Historically, this screening has been referred to as the “Range Safety COLA” process. In February 2010, United States Air Force (USAF) instruction AFI 91-217 was enacted, which mandated operational launch conjunction assessment/collision avoidance screenings by Air Force-controlled ranges. This AFI continued to require Range Safety COLAs but added LCOLA screens against on-orbit payloads and debris, this latter addition often called “Mission Assurance COLA” (MA COLA).

For NASA ELV launches, the Launch Services Program performed an analysis in July 2001 (ELVL-2001-0025354)[1] to determine the overall probability that a collision could occur during the launch phase. Various launch vehicles were examined in different orbit regimes, and the results indicated that the chance of hitting an on-orbit object during the relatively short launch phase is so small that Mission Assurance COLA measures have essentially no effect on overall mission success (It should be noted that at the time of the LSP analysis, the object catalog had significantly fewer tracked objects than the current catalogue). Following this study, LSP released a Program Directive (PD) on Collision Avoidance (LSP-PD-120.04), stating that Mission Assurance COLAs would not be routinely conducted for NASA LSP missions (this directive does not have any bearing on COLAs conducted by the appropriate launch range for every LSP mission). However, if LSP’s spacecraft customer requires a MA COLA analysis be performed, LSP must execute it as a formal mission requirement.

Under this LSP directive, NASA Jet Propulsion Laboratory (JPL) generally does not opt to perform any LCOLA screenings beyond the Range requirements. For many JPL missions, the launch window is either a very short duration or instantaneous. Additionally, many planetary or other deep-space missions have annual or even less frequent launch opportunities. These two factors combine to magnify the operational impact of standing down due to a low-risk conjunction.

In contrast, LSP has been conducting MA COLAs for every Goddard Space Flight Center (GSFC) mission since February 2004. In Goddard Policy RequirementGPR 8000.1, GSFC set forth the policy that each mission shall perform a MA COLA assessment against all on-orbit active satellites; no screening is required against on-orbit debris or spent upper stages. The objective of the GSFC policy is to protect orbiting assets, not necessarily the payload being launched.

Table 1 below summarizes the screening criteria used for the Air Force Ranges (per AFI 91-217) and the GSFC Policy. Both policies include provisions for P_c and miss distance criteria. It is clear that guidance differs significantly among the different organizations for both preferred/acceptable screening practices and associated thresholds.

Table 1. Summary of the Range and GSFC LCOLA Screening Criteria

	Manned - Range	Payloads - Range	Debris - Range	Payloads - GSFC
Probability of Collision	$1x10^{-6}$	$10x10^{-6}$	$10x10^{-6}$	$1x10^{-6}$
Miss Distance (Ellipsoidal)	200 x 50 x 50 km	Not used	Not used	Not used
Miss Distance (Spherical)	200 km	25 km	2.5 km	5 km
NASA Waiver	Not allowed	NA	NA	$3x10^{-5}$ cumulative (prior to launch day)
LDA Waiver	Not allowed	100×10^{-6} / 2.5 km	100×10^{-6} / 0.25 km	Not allowed
NAF/CC Waiver	Not allowed	$1{,}000 \times 10^{-6}$ / **	$1{,}000 \times 10^{-6}$ / **	Not allowed
MAJCOM/CC Waiver	Not allowed	$10{,}000 \times 10^{-6}$ / **	$10{,}000 \times 10^{-6}$ / **	Not allowed

Launch Collision Avoidance Issues

As the various LCOLA policies and implementation methods illustrate, there are no commonly accepted best practices among the agencies. The USAF policy serves to limit orbital debris, uses the SP catalog, and restricts the use of the P_c method due to their concern about unrealistic launch vehicle covariances. The GSFC policy serves to be a good steward and protect on-orbit assets, uses the GP catalog (with covariances estimated from empirical GP error growth information), and exclusively uses the P_c method in response to the inherent limitations of the miss distance method. Furthermore, in cases when similar methods are used, different criteria are employed with little or no rationale for how the criteria have been established.

While the commissioned NASA study, expected to be fully complete in early 2013, attempts to address nearly all of these issues, the items addressed in the present paper focus on three foundational issues:

- What are the actual errors in pre-launch trajectory estimates for common NASA launch vehicles?
- How do these errors compare to those of on-orbit space objects? What level of space catalogue precision is therefore appropriate for LCOLA screenings?
- What is the fidelity of the error statements (covariances) that accompany pre-launch estimated trajectories? Can they serve as a reasonable basis for P_c calculations?

The first two bullets above will be addressed in the next section and the final bullet in the section that follows, after which point certain conclusions will be drawn.

PRE-FLIGHT PREDICTED TRAJECTORY ERRORS

Launch conjunction assessment, as stated in the previous section, is presently only a lightly-standardized activity in which different indices and launch window closure criteria are used at different launch agencies and centers. However, regardless of the particular calculation and associated window closure approach, the so-called “miss distance,” or the vector magnitude of the position vector difference between the predicted launch trajectory and a conjuncting object, figures prominently in the computation; and in some cases this miss distance itself is the parameter of interest. As such, it is important to gain some understanding of the overall errors in the predicted launch trajectories, as these errors affect how a miss distance value should be interpreted. Additionally, the size of these errors will indicate whether analytic orbit models, such as the Simplified General Perturbations Theory #4 (SGP4), are adequate to the calculations for the LCOLA process or whether high-precision satellite catalogues should be employed.

The launch pre-flight predicted trajectories against which collision avoidance screenings are run consist of state estimates (position and velocity information) and covariance data at regular time intervals, typically three-second intervals, with the data beginning from three to thirty seconds after launch and continuing until approximately two hours after launch, although the actual durations are mission-specific. The state estimates are provided in the Earth-Fixed Greenwich (EFG) coordinate reference frame, primarily for the ease of trajectory adjustment when modifications to the nominal launch time are required. The furnished covariance information is the lower-triangle of the position covariance in the UVW (radial, in-track, cross-track) reference frame. This covariance information is derived from an uncertainty apportionment model that begins with the expected uncertainty in each of the physical components that govern spacecraft position (thrusters, gyros, &c.) as measured in the laboratory and combines all of these uncertainty data to synthesize an overall anticipated trajectory uncertainty at each time point. In some sense these covariance data are provided as a courtesy, as there appears to be no actual "realism" requirement levied on these error representations. The examination of the realism of these error representations is addressed in a later section.

The statement of trajectory "truth" against which these pre-flight trajectories can be evaluated is the actual flight trajectory telemetry data collected during each launch event. These groups of telemetry data for the missions under analysis were obtained by KSC and converted into a format convenient for analysis: individual position and velocity measurements of the spacecraft (from on-board GPS instruments), rendered in the Earth-Centered Inertial (ECI) True-of-Date reference frame, captured at typically one-second intervals. While this increased data density (increased, that is, over the three-second intervals in the predicted trajectory data) is certainly welcome, it is tempered somewhat by frequent data drop-outs. These drop-outs are due to lack of continuous ground-station coverage and other communications-related difficulties; and while they are more frequent and severe before TDRSS-enabled communication became more widespread, they remain common throughout the five-year period over which trajectories were analyzed.

In comparing the pre-flight trajectories to the associated telemetry in order to determine trajectory errors, a number of issues arise. First, the telemetry data lack any sort of accompanying error statement, either point-by-point or a single overall value (such as a standard error). In order to use the data, one is required essentially to presume that the telemetry data represent error-free truth. One hopes, of course, that the errors in the telemetry data are substantially smaller than those of the pre-flight trajectories so that the failure to account for the telemetry errors will not affect results. One will be better able to evaluate the rectitude of this assumption when the actual sizes of the trajectory errors are determined, as one can form some general opinions about the expected magnitude of GPS-derived position errors inherent in flight telemetry.

Second, the time points of the pre-flight and telemetry data do not align precisely; so in order to compare the two datasets some sort of interpolation must be performed. The interpolation of telemetry points suggests itself as the better choice, as the spacing of the telemetry data is more frequent and because this approach would eliminate the need to interpolate covariance information. Nonetheless, the interpolation of the telemetry still needs to be performed with caution due to the aforementioned telemetry drop-outs: a simple-minded interpolation scheme that improperly attempts to interpolate over non-trivial data-gaps will produce extremely inaccurate results in such situations. The telemetry interpolation methodology must be robust enough to recognize such data gaps and avoid them, and the approach adopted here is to require that each of the two interpolation boundaries be within five seconds of the predicted point. Distances outside of this range are considered to constitute a data gap and thus are not included in the analysis.

Third, pre-flight telemetry and associated covariance information comes with a particular predicted launch time. In the majority of the cases the predicted launch time differs from the actual launch time, the difference between the two launch times is usually small—less than one second—but it can sometimes be on the order of multiple minutes. The question is whether the actual or the predicted launch time should be used for accuracy analysis. The actual launch time scenario represents the trajectory situation as was actually flown, whereas the predicted launch time represents the situation as was actually screened. The decision was made to use the predicted launch time, as this situation represents the actual errors that made their way into the screening process.

As mentioned in the introduction, data were made available and analyzed for thirty-six prelaunch trajectories, comprising twenty-three Delta II, eleven Atlas V, and two Pegasus trajectories. In some cases partial information was available for other missions, but it is only these thirty-six that had sufficient, consistent data to merit direct use in the analysis. The launches represented a considerable variety of orbit types, although both pre-launch trajectory and telemetry data exist for only the first two to three hours of each event; so all analysis remained within the near-Earth orbit regime (that region of orbital space for which orbital periods are less than 225 minutes).

Position comparison was made for each point where comparisons were possible; drop-out periods were simply not analyzed. While it is possible that data dropouts could have systematically excluded certain levels of trajectory error, the lack of a pattern in the drop-outs' temporal location and duration makes this unlikely and suggests the permissibility of straightforward exclusion of the drop-out periods. Displaying the position difference data as an empirical cumulative distribution function (CDF) curve by individual mission allows the full distribution of the trajectory errors to be observed and thus more meaningful comparison among different trajectories. Additionally, the data were filtered by an altitude threshold of 400 km, as there is very little threat of close approach with space objects at altitudes lower than this (less than 5% of the space catalogue exists at such low altitudes, and apparently spurious trajectory error data appear at altitudes lower than this). Figures 1-3 represent the CDF plots of position errors for all three booster types (Atlas V, Delta II, and Pegasus). The legends spell out the particular missions used, and amplifying information for each mission is given in the appendix to this paper.

Figure 1 gives the position error results for all Atlas V launches. At the 50th percentile, nearly all Atlas V launches have errors greater than 10 km; and at the 95th percentile a little under half of them exceed 100 km.

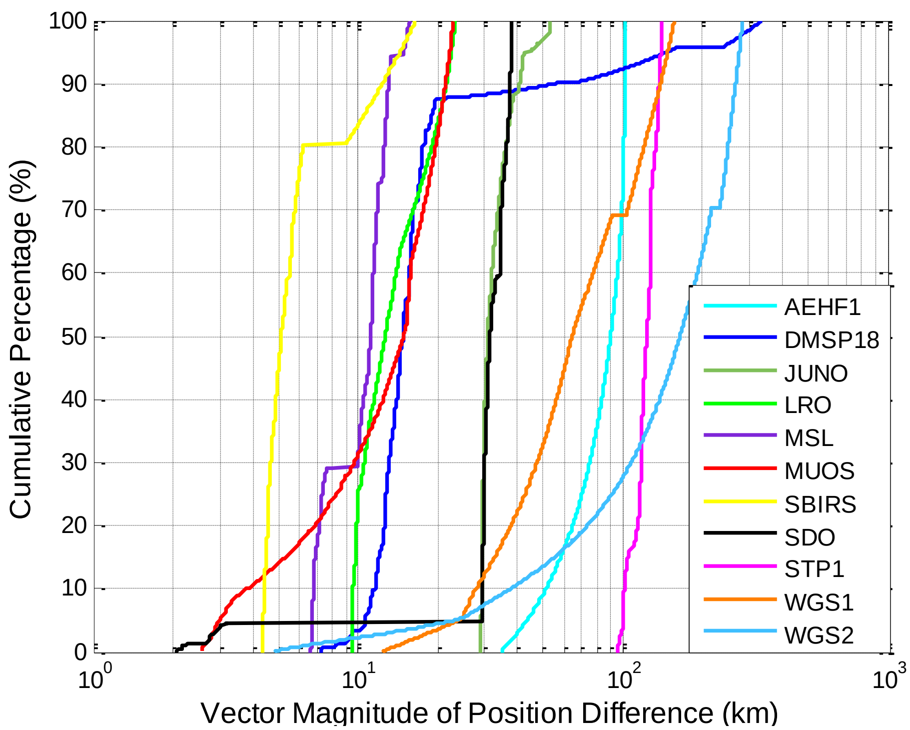

Figure 1: CDF plot of trajectory errors for all Atlas V launches

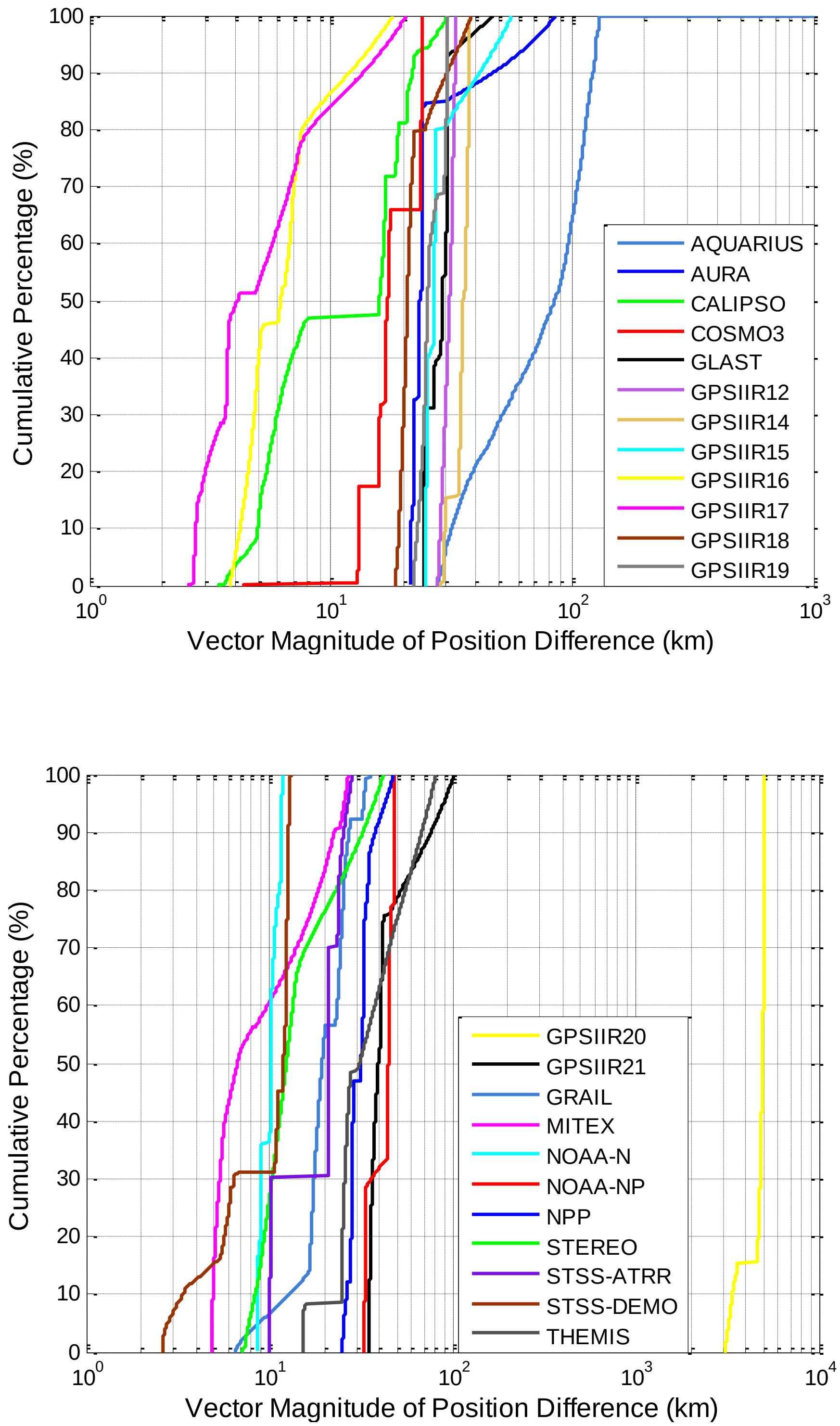

Figures 2a and b: CDF of trajectory errors for Delta II launches

Figures 2a and 2b give CDF representations of the position errors for the Delta II launches. On the whole, these show an error behavior that is somewhat more bounded than for the Atlas V, although the majority of trajectories show errors above 10 km at the 50th percentile. One trajectory, that of GPSII Flight 20, shows errors two orders of magnitude greater than all the others; and further examination was not able to determine any particular cause (*e.g.*, coordinate transformation problems). Because of its very different error character, this particular trajectory was judged to be anomalous and not considered in the remainder of the analysis.

Figure 3 represents the CDF plot of the position difference accuracy for Pegasus launches. There were paired pre-launch trajectory and telemetry data available for only three Pegasus missions; and all three of these were exceedingly short, with only a few minutes of total data in each. This is too little data from which to draw any durable conclusions, and as such the Pegasus trajectories are not used in the analyses of the subsequent sections; but as there is some interest in determining whether these solid-fuel motors seem to exhibit the same general error behavior as their liquid-fuel colleagues, the available data are presented here. The data for one of these trajectories never exceeded the 400 km altitude threshold and thus are not shown below; for the two others, what is available is plotted. If this abbreviated sample is truly representative of the entire error distribution, then one can conclude that the Pegasus error magnitudes and distribution are roughly similar to those for the Atlas V and Delta II launches.

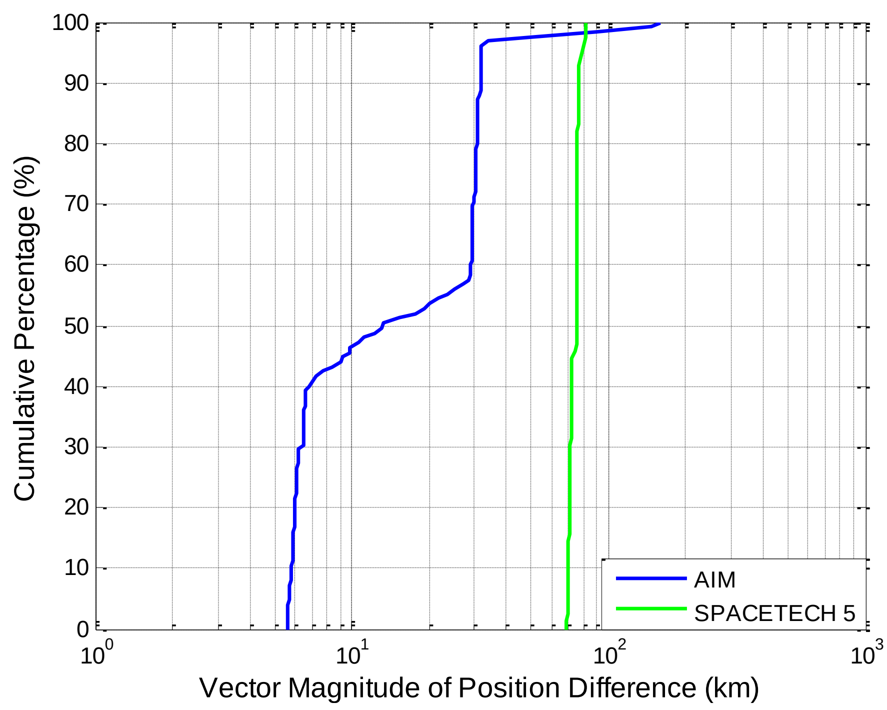

Figure 3: CDF of trajectory errors for Pegasus launches

Figures 1-3 give useful presentations of absolute error values and their distributions among the three different boosters analyzed, but it remains to put these error values in context; and the natural *comparandum* is the set of state estimate errors for on-orbit satellites. Such a comparison will also assist in determining the level of catalogue precision appropriate to the orbital safety evaluations of these trajectories.

The United States Strategic Command (USSTRATCOM) space catalogue comprises three distinct sub-catalogues of orbital information. The first is the Special Perturbations (SP) catalogue, which uses a higher-order orbital theory to produce a precision set of state estimates; these data are used internally for JSpOC processes and orbital safety calculations for satellites but are not generally circulated to external users. The second is the traditional General Perturbations (GP) catalogue, maintained with SGP4 orbit determination (OD), circulated to external users, and in recent times posted on www.space-track.org for anyone to download. There is, however, a new third option that is in beta testing now and is expected to transition within the next year to maintaining 75% or more of the GP catalogue: the so-called "extrapolation DC," or in some circles "eGP." This approach, described in detail in Cappellucci (2005),[2] takes a higher-order ephemeris (such as those from the SP catalogue) propagated into the future, creates synthesized observational data (called "pseudo-obs") from this ephemeris, and executes a GP OD from these synthesized data. Because the OD is fitting data derived from high-accuracy future predictions, the quality of the "predictions" using this approach is much better than the traditional, sensor-observations-based OD. Since the generally-available GP catalogue will be composed of these two types of GP OD approaches, a comparison of their errors to those of the pre-launch trajectories can serve both to ground the trajectory errors against some sort of benchmark and at the same time indicate whether the GP catalogue serves as an adequate basis for LCOLA calculations.

Figures 4-6 compare the errors in the launch trajectories to those of the publically-available portion of the satellite catalogue. In each of the figures, each CDF line is of a particular accuracy percentile value: in Figure 4, it is the 50th percentile, in Figure 5 the 68th percentile, and in Figure 6 the 95th percentile (these percentile values were chosen to remain analogous to the familiar percentile values for the mean, one-sigma, and two-sigma levels from a Gaussian distribution, even though vector error distributions do not in fact follow a Gaussian distribution). Because the construction of the graphic may be somewhat confusing, the following is a step-by-step account of the features in Figure 4, the 50th percentile accuracy CDF collection. For the Atlas V case, the 50th percentile error value from each of the eleven trajectories was calculated and a CDF curve constructed of these eleven values (red line); the same was done for the twenty-three Delta II (green line) and two Pegasus trajectories (pink line). For the satellite catalogue accuracy information, the data are derived from an analysis of all GP and eGP data for May 2012; and the 50th percentile values of a six-hour prediction (roughly equivalent to the amount of propagation used in LCOLA screenings) errors for each satellite were calculated and also summarized in CDFs. The precise method of calculating the satellite state estimate accuracies makes use of the reference orbits calculated for each satellite by the SuperCODAC accuracy estimation program that is presently part of the Astrodynamics Support Workstation (ASW) operational system; this methodology is described at length in Hejduk, Casali and Ericson (2005)[3] and Hejduk (2008).[4]

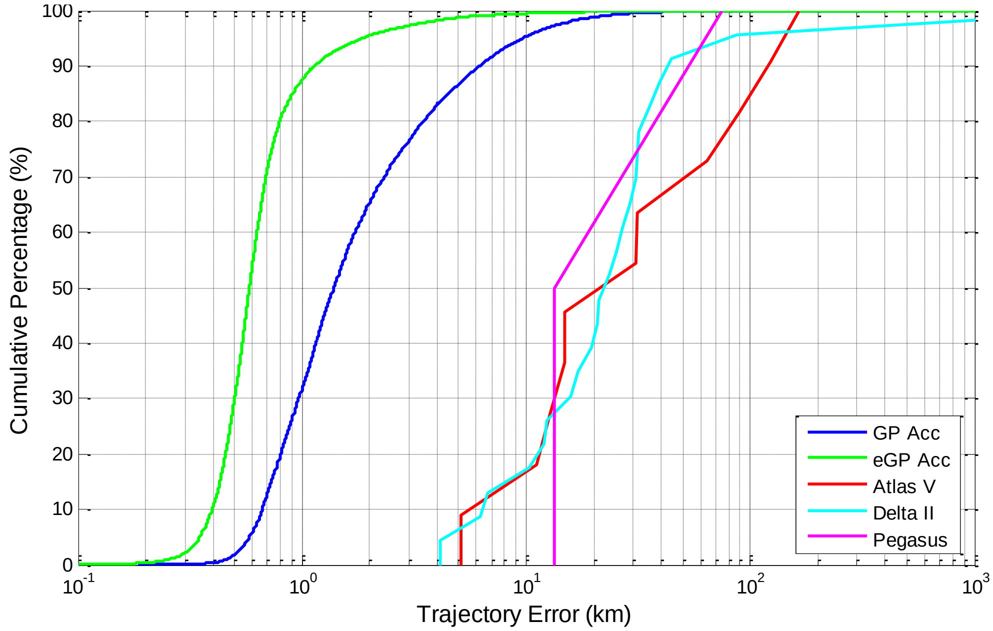

Figure 4: Launch / Satellite Accuracy Comparisons – 50th Percentile

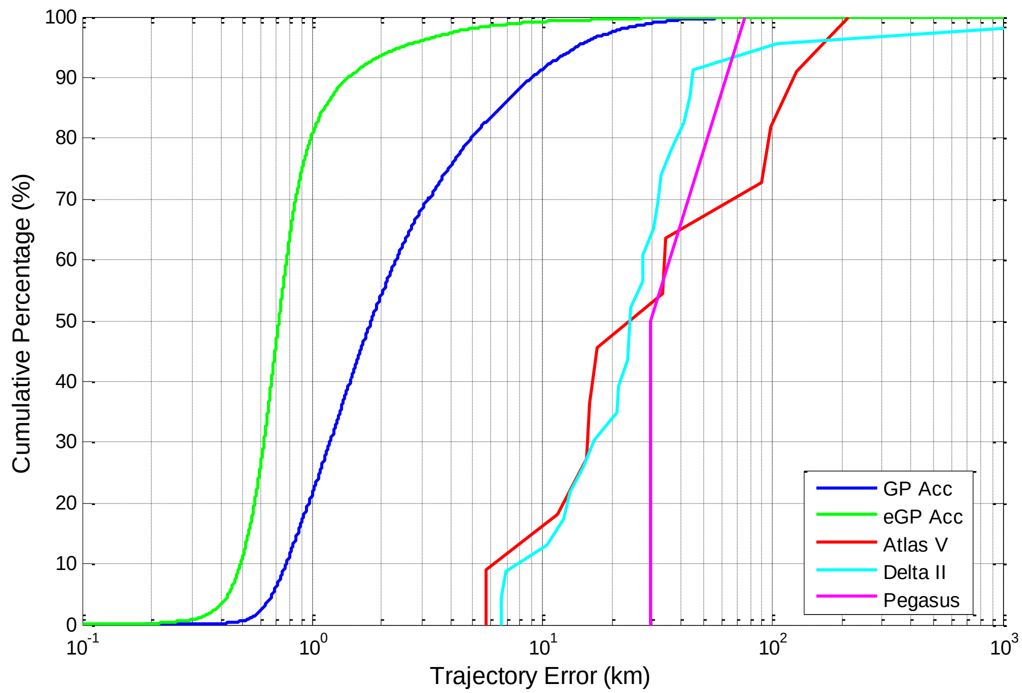

Figure 5: Launch / Satellite Accuracy Comparisons – 68th Percentile

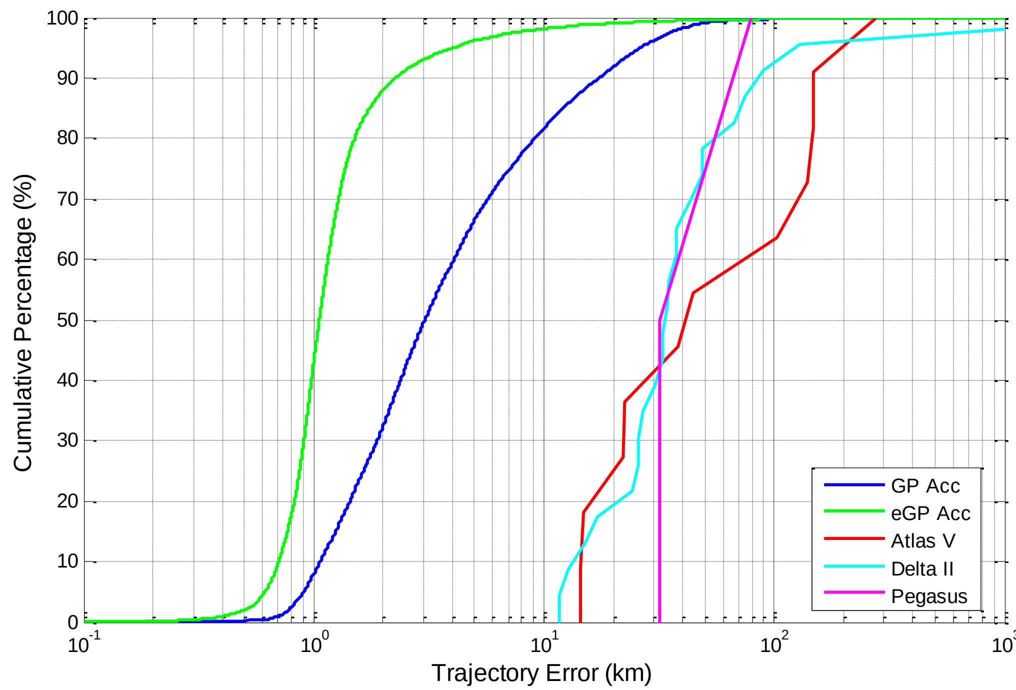

Figure 6: Launch / Satellite Accuracy Comparisons – 95th Percentile

In the 50th percentile graph (Figure 4), the pre-launch trajectory errors for most of the cumulative percentage span remain about an order of magnitude larger than the GP catalogue errors and about one and one-half orders of magnitude larger than the eGP errors. In the 68th and 95th percentile graphs, the difference is somewhat smaller but still hovers about an order of magnitude for much of the cumulative percentage span; this is especially so for the eGP data.

There are two conclusions one could draw from these data. First, because the satellite GP catalogue errors are consistently and substantially smaller than the pre-launch trajectory errors, it is clear that there will be little to no appreciable benefit from using the precision (SP) rather than the GP satellite catalogue for LCOLA screenings and risk assessment. It is true that in support of calculating probabilities of collision, actual OD covariance data generated and preserved with the precision catalogue can be used, whereas covariances must be estimated when using the GP catalogue; but in terms of accuracy levels alone, the inherent errors in the pre-launch trajectories are so much larger than the GP catalogue errors that if the precision catalogue is not conveniently available, there is little motivation to take on the difficulties of obtaining and using it for LCOLA.

One could also remark that the trajectory errors are so large in an absolute sense that orbital safety calculations will never be reliable enough to be actionable. This question is taken up in the latter phases of the NASA study, but one should point out immediately that it is not the absolute values of the trajectory errors *per se* but rather the harmony between them and their error characterization (covariance) that truly determines their utility. If the associated covariances adequately model the actual trajectory errors, then the initial gate is cleared: credible orbital safety calculations, especially that of the probability of collision, become possible. The next section addresses the reliability of launch covariance data to determine whether this initial condition can be met.

PRE-LAUNCH TRAJECTORY COVARIANCE REALISM

The previous section has shown that pre-launch trajectories do have large errors, certainly when compared to the state estimate errors of catalogued satellites; and to some degree this level of performance is disappointing, as smaller errors do very much assist in separating real from fallacious orbital safety events. However, the actual enabling factor for orbital safety calculations is not the accuracy of the predicted trajectory itself but rather the precision of the accompanying covariance, which is the characterization of this trajectory error: if the covariance is realistic, then a meaningful probability of collision (P_c) can be calculated for an event and decisions made accordingly. Some can object that predicted trajectories with very large errors and accompanying appropriately large covariances are not useful to the orbital safety mission because the large covariance "dilutes" the P_c to the point that the probabilities are so small that they are not actionable; and indeed groups, even sizeable ones, of low-probability events do leave decision-makers in an indeterminate position *vis-à-vis* risk assessment. But it must be remembered that if the covariance is realistic, the P_c is the actual probability of collision; and this outcome—the presence of a real P_c —is the necessary beginning for a meaningful orbital safety risk assessment. Said differently, if the covariance is not realistic, then there can be no meaningful P_c calculation and risk assessment; whereas if the covariance does accurately represent the error in the estimated trajectory, then there is at least the possibility of performing meaningful calculations and from them drawing risk conclusions. It is thus necessary to investigate the launch trajectory covariances to assess their success in statistically characterizing the trajectory errors.

Before beginning such an investigation, it must be recognized that the formulation of the covariance used for the launch trajectory errors (and, for that matter, with satellite state estimates as well) imposes certain limits to its serving as an error statement. The covariance provides only the second moment (the variance) for each of the state component errors (covariance diagonal) and the terms indicating the degree of correlation among these variances (covariance off-diagonal terms). Embedded in this somewhat laconic presentation are the presumptions that the mean error in each component is zero, so no statement of error bias is needed; and that the error distribution is such that it can be characterized by the second moment alone. Although there are a number of distributions that can be characterized by just two parameters, implicit here is the presuexpectation that the errors in each component will follow a normal (Gaussian) distribution. The examination of this presumption for satellite state estimation is an expanding research area with a considerable and growing of critical literature; many question the propriety of this presumption in propagation, but even in some cases at epoch (a good survey of this literature can be found in Ghrist and Plakalovic [2012]).[5] Because the form and framing of the covariance requires a Gaussian assumption, one will for the sake of this analysis simply accept it and not attempt to reevaluate it here; but the tests for covariance realism do implicitly make this assumption. If the tests pass, then it is verified both that the error distribution is at least approximately Gaussian and that the covariance properly represents this distribution; if they fail, one is left with a somewhat indeterminate situation in that either the underlying error distribution is not Gaussian, the distribution is not properly represented by the covariance, or both.

A position covariance, which is the portion of the matrix to be tested for proper error representation,[*] describes a three-dimensional distribution of position errors about the object's nominal

[*] The velocity portion of the covariance, as well as the elements for the other solved-for terms in the orbit determination (such as drag and solar radiation pressure), are not explicitly tested as part of this analysis because it is only the position portion of the covariance that is used for the P_c calculation and, more significantly, only the position portion is supplied as part of the launch data.

estimated state. The test procedure is to calculate a set of these state errors and determine whether their distribution matches that indicated by the position covariance matrix. To understand the particular test procedure, it is best to consider the problem first in one dimension, perhaps the in-track component of the state estimate error. Given a series of state estimates for a given trajectory and an accompanying truth trajectory, one could calculate a set of in-track error values, here given the designation ε, as the differences between the estimated states and the actual true positions. According to the assumptions previously discussed about error distributions, this vector of error values should conform to a Gaussian distribution. As such, one can proceed to make this a "standardized" normal distribution, as is taught in most introductory statistics classes, by subtracting the mean and dividing by the standard deviation

$$\frac{\varepsilon - \mu}{\sigma} \tag{1}$$

This should transform the distribution into a Gaussian distribution with a mean of 0 and a standard deviation of 1, a so-called "z-variable." Since it is presumed from the beginning that the mean of this error distribution is 0, the subtraction as indicated in the numerator of (1) is unnecessary, simplifying the expression to

$$\frac{\varepsilon}{\sigma} \tag{2}$$

It will be recalled that the sum of the squares of *n* standardized Gaussian variables constitutes a chi-squared distribution of *n* degrees of freedom. As such, the square of (2) should constitute a one-degree-of-freedom chi-squared distribution. This particular approach of testing for normality—evaluating the square of the sum of one or more z-variables—is a convenient approach for the present problem, as all three state components can be evaluated as part of one calculation (u representing the vector of state errors in the radial direction, v the in-track direction, and w the cross-track direction):

$$\frac{\varepsilon_u^2}{\sigma_u^2} + \frac{\varepsilon_v^2}{\sigma_v^2} + \frac{\varepsilon_w^2}{\sigma_w^2} = \chi^2_{3\,dof} \tag{3}$$

One could calculate the standard deviation of the set of errors in each component and use this value to standardize the variable, but it is the covariance matrix that is providing, for each sample, the expected standard deviation of the distribution; and since the intention here is to test whether this covariance-supplied statistical information is correct, the test statistic should be using the variances from the covariance matrix rather than a variance calculated from the actual sample of state estimate errors. For the moment, it is helpful to presume that the errors align themselves such that there is no correlation among the three error components (for any given example it is always possible to find a coordinate alignment where this is true, so the presumption here is not far-fetched; it is merely allowing that that particular coordinate alignment happen to be the UVW coordinate frame). In such a situation, the covariance matrix would look like the following:

$$C = \begin{bmatrix} \sigma_u^2 & 0 & 0 \\ 0 & \sigma_v^2 & 0 \\ 0 & 0 & \sigma_w^2 \end{bmatrix} \tag{4}$$

and its inverse is straightforward

$$C^{-1} = \begin{bmatrix} 1/\sigma_u^2 & 0 & 0 \\ 0 & 1/\sigma_v^2 & 0 \\ 0 & 0 & 1/\sigma_w^2 \end{bmatrix}. \tag{5}$$

If the state errors are formulated as

$$\varepsilon = [\varepsilon_u \quad \varepsilon_v \quad \varepsilon_w] \tag{6}$$

then the pre-and post-multiplication of the covariance matrix inverse by the vector of errors, as shown in (5), will produced the desired chi-squared result:

$$\varepsilon C^{-1} \varepsilon^T = [\varepsilon_u \quad \varepsilon_v \quad \varepsilon_w] \begin{bmatrix} 1/\sigma_u^2 & 0 & 0 \\ 0 & 1/\sigma_v^2 & 0 \\ 0 & 0 & 1/\sigma_w^2 \end{bmatrix} \begin{bmatrix} \varepsilon_u \\ \varepsilon_v \\ \varepsilon_w \end{bmatrix} = \frac{\varepsilon_u^2}{\sigma_u^2} + \frac{\varepsilon_v^2}{\sigma_v^2} + \frac{\varepsilon_w^2}{\sigma_w^2} = \chi^2_{3dof} \tag{7}$$

What is appealing about this formulation is that, as the covariance becomes more complex and takes on correlation terms, the calculation procedure need not change: the matrix inverse will formulate these terms so as to apportion the variances properly among the U, V, and W directions, and the chi-squared variable can still be computed with the $\varepsilon C^{-1} \varepsilon^T$ formulary.

This procedure is easily applied to the dataset in possession: the pre-launch data comprise a state estimate and covariance for each point in the trajectory, and the flight telemetry data provide a truth criterion; so the calculation in (7) could be computed for every pre-launch data point and that entire dataset examined for conformity to a three-dof chi-squared distribution. Such an approach, however, would have multiple drawbacks: it would fall victim to the obvious correlation between closely-spaced data points, it would not account for the fact that different trajectories have different lengths (and thus more heavily weight the longer trajectories), and it would not take cognizance of the fact that different phases of a launch may have different error characteristics and thus different covariance realism results. To mitigate these difficulties, the following procedure was assembled. First, the Atlas V and Delta II trajectories were analyzed separately (there were not enough Pegasus data to allow an investigation of their trajectories' covariance realism). Second, an interval of five minutes between analyzed points was maintained in order to attenuate correlation between points; this means that, for example, all of the 5-minute points for the Atlas V trajectories were evaluated together, all of the 5-minute points for the Delta II's, all of the 10-minute points for the Atlas V's, all of the 10-minute points for the Delta II's, &c. Finally, even though there are 11 Atlas V and 23 Delta II trajectories in the dataset, because of drop-outs there are not necessarily that number of data points at each 5-minute boundary point; so for certain statistical analyses a minimum number of data points was imposed in order to consider a particular trajectory / time-point pair.

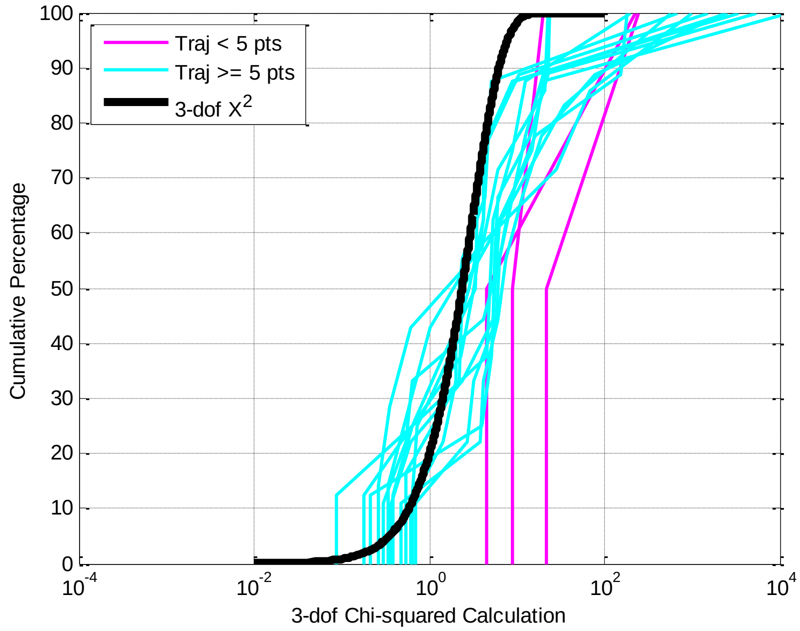

Figure 7: Atlas V trajectories: 15-90 minutes, at 5-minute intervals

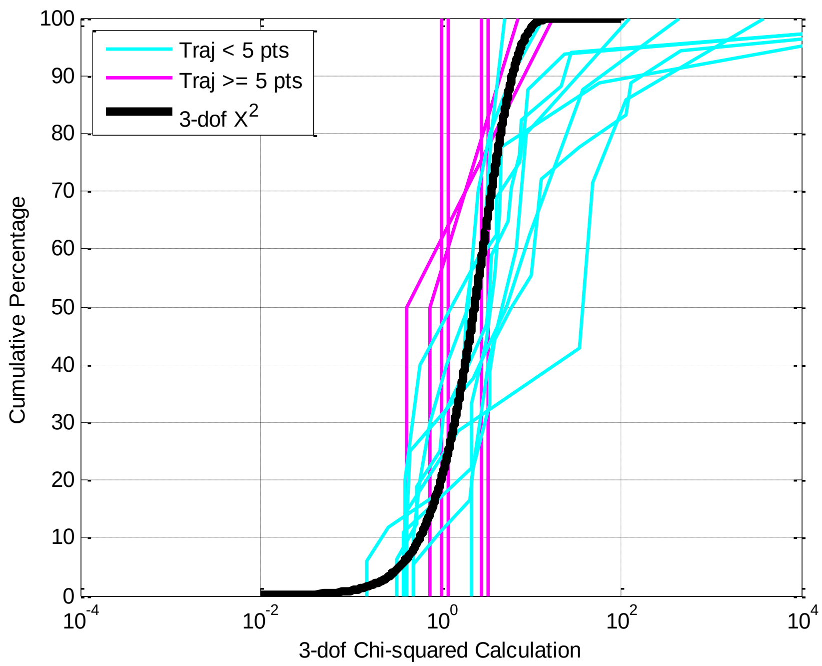

Figure 8: Delta II trajectories: 15-90 minutes, at 5-minute intervals

Figures 7 and 8 show the results, for the Atlas V and Delta II trajectories, of the CDF-plotting of the chi-squared results from each trajectory time point; here, five-minute intervals from 15 to

90 minutes were used, resulting in a total of sixteen trajectories for each. Those trajectory time-points that had fewer than five points, and thus more difficult to interpret in terms of their CDF behavior, are shown in magenta; those with five or more points are shown in aqua; and the ideal three-degree-of-freedom chi-squared CDF is given as a thick black line. One can see that for both trajectories, the CDF curves, especially the aqua ones, are reasonably similar to the ideal black line. Each booster group included one trajectory with especially large chi-squared values (probably resulting from unusually large trajectory errors that were much larger than the accompanying covariances would suggest); if these two trajectories were excluded from the analysis, the performance would improve considerably in the upper tails of the CDFs, which is where the most divergence is observed. But rather than exclude these based on their poor performance alone, it is best to let them remain in the analysis for the present and remove them only if a reasonable case can be made for such exclusion later.

It is encouraging, certainly, that there is a considerable degree of visual alignment between the ideal and empirical distributions, but this sort of "ocular regression" is hardly conclusive; what is needed is a rigorous statistical test to determine whether these empirical distributions can be considered to be associated with a chi-squared parent distribution. Such a desire leads the investigation to the statistical sub-discipline of "goodness of fit" (GOF).

Every student of college statistics learns about "analysis of variance" (ANOVA), the particular procedure for determining whether two groups of data can essentially be considered to be describing the same or different phenomena. More precisely, it is a procedure for determining whether the experimental distribution, produced by the research hypothesis, can be considered to come from the parent distribution represented by the null hypothesis; and the operative statistic arising from the analysis is the *p-value*: the likelihood that the research hypothesis is a sample drawn from the null hypothesis's parent distribution. If this value becomes small, such as only a few percent, it means that there are only, say, two or three chances in one hundred that the differences between the two samples (null and research) can be explained by sampling error alone, which in this case would be likely to lead to the rejection of the null hypothesis and the embrace of the research hypothesis. This procedure is a specific example of statistical hypothesis testing.

A similar procedure can be applied to evaluate GOF, namely, to evaluate of how well a sample distribution corresponds to a hypothesized parent distribution. In this case, the general approach is the reverse of the typical ANOVA situation: it is to posit for the null hypothesis that the sample distribution does indeed conform to the hypothesized parent distribution, with a low p-value result counseling the rejection of this hypothesis. This approach does favor the association of the sample and the hypothesized distribution, which is why it is often called "weak-hypothesis testing"; but that is not necessarily an unreasonable method: what is being sought is not necessarily the "true" parent distribution but rather an indication of whether it is reasonable to propose the hypothesized distribution as the parent distribution. Such a view is appropriate to the present purpose, namely whether the behavior of the CDFs for individual time-points in the trajectories of certain booster types can be reasonably ascribed to a 3-dof chi-squared parent distribution.

There are several different mainstream techniques for goodness-of-fit weak-hypothesis testing: moment-based approaches, chi-squared techniques (not in any way linked to the fact that the present application will be testing for conformity to a chi-squared distribution), regression approaches, and empirical distribution function (EDF) methods. Of all of these, the EDF methodology is generally considered to be both the most powerful and most fungible to different applications, so it is the one selected for use here. The general EDF approach is to calculate and tabulate the differences between the CDF of the sample distribution and that of the hypothesized distribution, to calculate a GOF statistic from these differences, and to consult a published table of p-values for the particular GOF statistic to determine a significance level. Specifically, there are two GOF statistics in use with EDF techniques: supremum statistics, which draw inferences from the greatest single deviation between the empirical and idealized CDF (the Kolmogorov-Smirnov statistics are perhaps the best known of these); and quadratic statistics, which involve a summation of a function of the squares of these deviations (the Cramér – von Mises and Anderson-Darling statistics are the most commonly used). It is believed that the quadratic statistics are the more powerful approach, especially for samples in which outliers are suspected; so it is this set of GOF statistics that were employed for the present analysis. The basic formulation for both the Cramér – von Mises and Anderson-Darling approaches is of the form

$$Q = n\int_{-\infty}^{\infty}\left[F_n(x) - F(x)\right]^2 \psi(x)dx \ ; \tag{8}$$

the two differ only in the weighting function ψ that is applied. The Cramér – von Mises statistic is the simpler:

$$\psi(x) = 1 \tag{9}$$

setting ψ to unity; the Anderson-Darling is the more complex, prescribing a function that weights data in the tails of the distribution more heavily than those nearer the center:

$$\psi(x) = \{F(x)[1 - F(x)]\}^{-1} \tag{10}$$

Because it is already suspected that each booster type has a single trajectory that is an outlier in the upper tail, it is appropriate to choose the Cramér – von Mises statistic for this investigation.

It is a straightforward exercise to calculate the statistic in (8), discretized for the actual individual points in the CDF for each trajectory (that is, changing the integral into a summation). This calculates the Cramér – von Mises statistic, from this point on called the "Q-statistic," as suggested in (8). The step after this is, for each Q-statistic result, to consult a published table of p-values, determined by Monte Carlo studies, for this test to determine the p-value associated with each Q-statistic.[6] The usual procedure is to set a p-value threshold (*e.g.*, 5%, 2%, 1%) and then to determine whether the sample distribution produces a p-value greater than this threshold (counseling the retention of the null hypothesis: sample distribution conforms to hypothesized distribution) or less than this threshold (counseling rejection of the null hypothesis: sample distribution cannot be said to derive from the hypothesized distribution as a parent). In the present case, the p-value table instead will be interpolated to determine the p-value level associated with each tested time-point, and the p-value results can then themselves be plotted as a CDF.

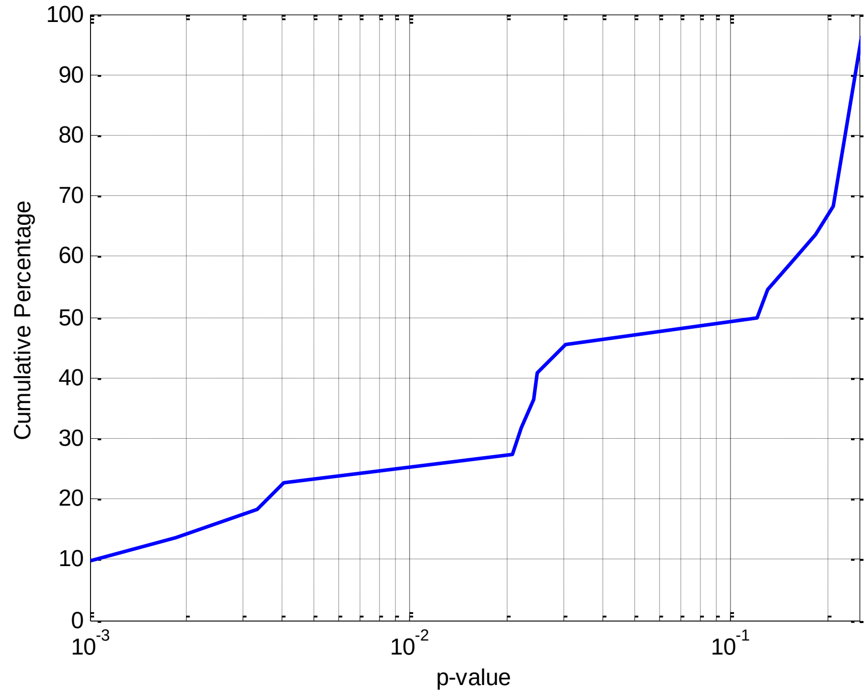

Figure 9: p-value results for all trajectories, time points 15-90 minutes, > 5 samples

Figure 9 gives the p-value results, with outcomes from all trajectory time points (with at least five data points) all mixed together. The boundaries of the graph are set at the boundaries of the published p-value tables (0.1% to 25%), so intersections with the vertical axes indicate percentages of the dataset that were not directly evaluatable but yet can still be interpreted (either bad enough to constitute unhesitating rejection of the null hypothesis or at a level at which there would be uniform acceptance of the null hypothesis).

In understanding these results, it is helpful to keep in mind that a p-value range of 2% to 5% is typical for retaining the null hypothesis in a goodness-of-fit evaluation, meaning that values greater than this would indicate that the sample could be considered to derive from the hypothesized parent distribution, in this case a 3-dof chi-squared distribution. From Figure 9 one can observe that a little more than 50% of the cases exceed a p-value of 5% (0.05) and about 75% exceed a p-value of 2% (0.02). This is a very encouraging result: 75% of the cases examined pass outright, without any outlier exclusion or manipulation, a GOF text for the hypothesized distribution. If one were to be more permissive and allow a result of 0.1%, which is the boundary for the published tables, then 90% of the results would pass the GOF test.

It would be unreasonable to expect that all of the results of such an examination, especially given the vicissitudes of actual operational data production, would conform to the idealized case; so the fact that 75% of such cases pass the GOF test at a commonly-chosen p-value threshold is quite significant, and that this can be extended to 90% through a somewhat more lenient application of the test. Furthermore, since it is not certain that in all cases individual component errors would follow a Gaussian distribution, these results are all the more impressive. It can be said that the covariances supplied with the launch trajectories do indeed accurately represent the observed trajectory errors.

CONCLUSIONS AND FUTURE WORK

The first part of the NASA-sponsored LCOLA study covered herein sought to determine whether the launch-related data supplied for LCOLA operations are adequate to a reasonable performance of that mission; and the conclusion advanced here is that they are. The trajectory errors are large when compared to typical on-orbit satellite state estimate errors, but the fact that the covariances appropriately reflect those errors allows a credible P_c to be calculated and the LCOLA process to be properly enabled. The large errors do allow the GP space catalogue to be adequate to the LCOLA task, presuming covariances can be estimated appropriately from historical GP error information. Use of the precision catalogue will certainly do no harm, but it is not strictly necessary for this mission.

Of course, what is established here is merely foundational—that the present launch data can form an adequate basis for LCOLA; it remains to examine and form recommendations regarding particular calculation/screening procedures and launch window closure thresholds. The second part of the NASA study pursues this through a large experiment in which five representative launch trajectories were subjected to a very large number of screenings (one-minute intervals from -15 to +15 days from the nominal launch time, or 43,200 screenings per trajectory), in both GP and SP modes, to determine P_c distributions, miss distance distributions, maximum versus cumulative P_c comparisons, and GP versus SP comparisons. This dataset has been very helpful in suggesting recommendations for all of the parameters listed above. It is expected that these results will be assembled into a follow-on conference paper and presented at the upcoming AAS summer meeting.

APPENDIX: TABLE OF FLIGHT TRAJECTORIES AND THEIR ACCURACIES

#	Mission Name	Launch Date	Booster Type	50th Percentile	68th Percentile	95th Percentile
1	AEHF – 1	Aug-14-2010	Atlas V	89.95	98.59	101.94
2	DMSP 18	Oct-18-2009	Atlas V	14.80	16.05	147.47
3	JUNO	Aug-05-2011	Atlas V	30.89	33.48	44.71
4	LRO	Jun-18-2009	Atlas V	12.69	15.63	22.49
5	MSL	Nov-26-2011	Atlas V	11.13	11.72	14.87
6	MUOS	Feb-24-2012	Atlas V	14.87	17.24	22.23
7	SBIRS	May-07-2011	Atlas V	5.13	5.67	14.41
8	SDO	Feb-11-2010	Atlas V	31.53	34.53	38.00
9	STP – 1	Mar-08-2007	Atlas V	123.21	127.32	139.14
10	WGS – F1	Oct-11-2007	Atlas V	64.47	89.38	147.96
11	WGS – F2	Apr-04-2009	Atlas V	164.60	211.89	275.66
12	GLAST	Jun-11-2008	Delta II	28.97	30.21	35.06
13	GPS – IIR12	Jun-23-2004	Delta II	31.07	31.88	32.88
14	GPS – IIR14	Sep-26-2005	Delta II	35.36	36.71	37.54
15	GPS – IIR15	Sep-25-2006	Delta II	26.91	27.13	48.92
16	GPS – IIR16	Nov-17-2006	Delta II	6.21	6.97	15.03
17	GPS – IIR17	Oct-17-2007	Delta II	4.11	6.58	17.14
18	GPS – IIR18	Dec-20-2007	Delta II	20.76	21.44	34.35
19	GPS – IIR19	Mar-15-2008	Delta II	25.22	27.51	30.52
20	GPS – IIR20	Mar-24-2009	Delta II	4,915.92	5,003.52	5,067.46
21	GPS – IIR21	Aug-17-2009	Delta II	39.36	41.36	89.52

22	GRAIL	Sep-10-2011	Delta II	19.41	24.30	32.76
23	MITEX	Jun-21-2006	Delta II	6.72	13.20	25.67
24	STEREO	Oct-26-2006	Delta II	12.39	14.98	37.33
25	STSS – DEMO	Sep-25-2009	Delta II	11.94	12.42	12.82
26	THEMIS	Feb-17-2007	Delta II	31.14	43.72	74.71
27	AQUARIUS	Jun-09-2011	Delta II	86.44	104.81	128.65
28	AURA	Jun-15-2004	Delta II	23.39	23.87	67.13
29	CALIPSO	Apr-28-2006	Delta II	15.90	16.86	25.82
30	COSMO – 3	Oct-25-2008	Delta II	17.15	23.61	24.11
31	NOAA – N	May-20-2005	Delta II	10.25	10.54	11.69
32	NOAA – N’	Feb-06-2009	Delta II	44.66	45.35	48.47
33	NPP	Oct-28-2011	Delta II	31.74	32.90	42.89
34	STSS – ATRR	May-05-2009	Delta II	21.05	21.19	26.87
35	AIM	Apr-25-2007	Pegasus	13.28	29.56	31.80
36	SPACETECH5	Mar-22-2006	Pegasus	74.83	75.22	79.39

REFERENCES

[1] Need full study citation here

[2] Cappellucci, D.A. “Special Perturbations to General Perturbations Extrapolation Differential Corrections in Satellite Catalog Maintenance.” AAS/AIAA Astrodynamics Specialists Conference (Lake Tahoe, CA), Aug. 2005.

[3] Hejduk, M.D., Ericson, N.L., and Casali, S.J. “Beyond Covariance: A New Accuracy Assessment Approach for the 1SPCS Precision Satellite Catalogue.” 2006 MIT / Lincoln Laboratory Space Control Conference, Bedford, MA. May 2006.

[4] Hejduk, M.D. “Space Catalogue Accuracy Modeling Simplifications.” 2008 AAS Astrodynamics Specialists Conference, Honolulu, HI, August 2008.

[5] Ghrist, R.W. and Plakalovic, D. “Impact of Non-Gaussian Error Volumes on Conjunction Assessment Risk Analysis). AAS/AIAA Astrodynamics Specialists Conference (Minneapolis, MA), Aug. 2012.

[6] D’Agostino, R.B. and Stephens, M.S. Goodness-of-Fit Techniques. New York: Marcel Dekker, 1986.